# Single Anchor-Based Infrastructure-less Localization Performance using UWB Radios

Shashank Bhushan, Ashish Ahluwalia, Ashutosh Deshwal, Amitangshu Pal Computer Science and Engineering, Indian Institute of Technology Kanpur, Kanpur, UP, India Email: [sbhushan21,ashisha21,ashutoshd22,amitangshu]@iitk.ac.in

Abstract—The paper discusses single anchor-based solutions for providing infrastructure-less localization using Ultra Wide Band (UWB) radios. The localization solution proposed in this paper comprises of two essential components: a fixed anchor node, which serves as the base station, and one or more mobile tags. The anchor and the tags are equipped with two UWB modules in orthogonal directions – with this setup, the proposed solution is capable of accurately measuring the distance and the angles between the anchor and the tags in a 3D plane. Through extensive experimentation, we show that the proposed solution achieves a ranging error well below 1 m, whereas the angle measurement errors lie below 10°.

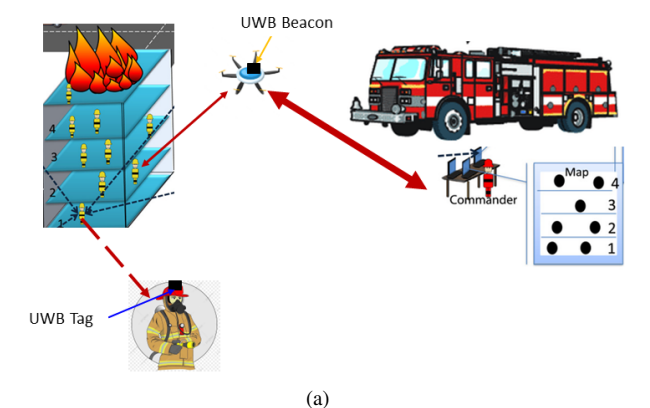
Index Terms—Infrastructure-less localization, Ultra Wide Band Radios, Two Way Ranging, Angle-of-arrival

## I. INTRODUCTION

Indoor localization research encompasses a wide range of applications, including tracking individuals in complex indoor spaces, monitoring the movement of wearable devices or mobile robots, optimizing resource allocation in industrial settings, improving emergency response, enhancing user experiences in retail environments, and enabling seamless navigation in large venues such as airports or shopping malls. Various techniques of indoor localization have been developed, such as Inertial Measurement Unit (IMU) based indoor localization [1], simultaneous localization and navigation (SLAM) [2], triangulation or multilateration using multiple anchors/beacons [3] etc. However, these techniques have their own drawbacks. For example, the IMU sensor-based localization solutions suffer from poor accuracy, whereas other solutions require some existing infrastructure (such as multiple anchors/beacons) to be in place. In this paper, our objective is to explore localization in infrastructure-free environments using a single anchor node.

# A. Some applications of single anchor-based localization

We now discuss the primary motivation and some application areas for studying single anchor-based localization (SAL). Two primary areas where SAL can find applications are during (a) search & rescue missions, or (b) hostage rescue operations and house interventions. Often time the rescue personnel in search & rescue operations (like firefighters) get trapped inside buildings [4]–[6], and quickly finding them becomes challenging. On the other hand, during the hostage rescue operations and house interventions it also becomes essential to quickly identify and evacuate the wounded security forces in order to provide them with prompt medical care [7]. However, the quick rescue operations are seriously



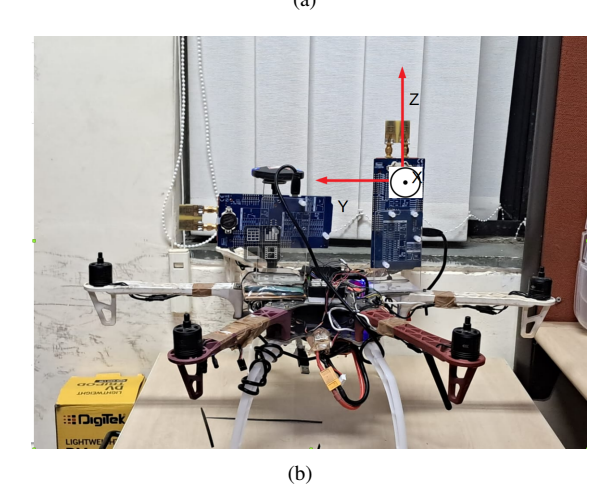


Fig. 1: (a) A conceptual illustration of SAL in a mission-critical application, where (b) the radios can be mounted on some fire-trucks or drones. These fire-trucks or drones can then work as anchor nodes to locate the tags that are mounted on the rescue team.

hampered by the absence of a reliable localization or tracking mechanism. Therefore, often time the rescue team faces a lot of difficulty in getting to the injured individuals swiftly and removing them from hostile situations.

One such scenario where a single anchor-based portable system can be used is illustrated in Fig. 1, which involves equipping the rescue personnel with RF devices, that can be attached to their helmets. Additionally, a drone carrying a similar RF device (which works as an anchor/beacon node) can be deployed and operated by the base station commander. The anchor node can also be mounted on the firetrucks or police vans, and is equipped with GPS. This anchor node then serves the purpose of locating and tracking the rescue personnel in the affected area. At the central station, the

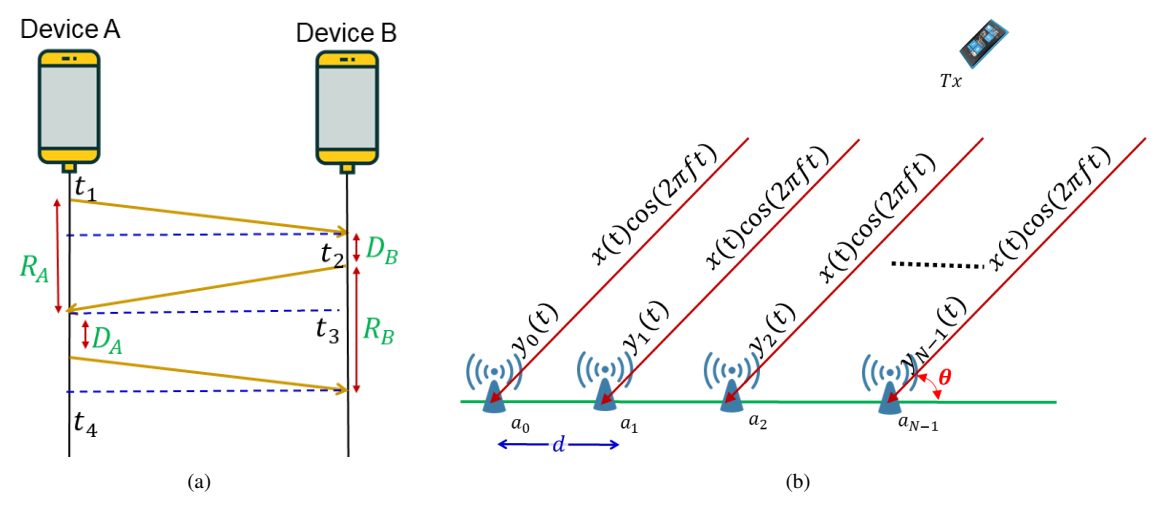


Fig. 2: Illustration of the (a) TWR, and (b) AoA measurement technique.

received location information is processed and displayed on the computers for further processing.

## B. Existing localization techniques and their limitations

Over the past several decades, extensive research has been conducted in this field. Typically, two categories of solutions are utilized: the first one is IMU-based where sensors like accelerometers, gyroscopes, and magnetometers are used to detect changes in an object's position or orientation w.r.t. its initial position, whereas the second one uses RF signals and/or computer vision solutions to provide precise object position or orientation data relative to some fixed reference points. Below we summarize these techniques and their limitations.

IMU-based solutions: IMU-based indoor localization has been a very well-researched area. These IMU sensors can be integrated into clothing and shoes of a person for the purpose of real-time tracking [8], [9]. On the other hand, smartphones equipped with built-in IMUs have also been leveraged for indoor localization, employing modified Kalman filters [10]. Another indoor localization system utilizing IMU and photodiode sensors in smartphones is demonstrated in [11]. A pedestrian dead reckoning system utilizing a chest-mounted IMU is proposed in [12]. Another study based on multiple neural networks tailored to user orientation for improved indoor user tracking is studied in [13]. However, the primary drawback of the IMU sensors is poor accuracy, due to the accumulation of errors and drifts over time.

**RF-based solutions:** Several studies have explored RF-based positioning techniques using passive UHF RFID, Bluetooth, and WLAN radios for tracking mobile systems [14]. Wi-Fi fingerprinting-based techniques have been extensively studied in the literature [15], [16], however, these techniques require an extensive data collection phase and are not adaptive to environmental changes. The authors in [17] have used the random forest algorithms for the Non-Line-of-Sight (NLOS) identification for indoor localization. Kinect cameras have also been effectively used for indoor robot navigation, utilizing depth data and error minimization techniques, although

challenges with dynamic obstacles persist [18]. Recently, Ultra-Wideband (UWB) localization techniques using triangulation with time of arrival (ToA), angle of departure (AoD), and angle of arrival (AoA) data have excelled in many diverse environments [19]–[24].

**Hybrid solutions:** Some hybrid indoor localization systems, merging IMU sensors and smartphone cameras, have shown enhanced accuracy while outperforming the individual methods [25]. Another study in [26] implements sensor fusion using RSSI and IMU data, employing the Extended Kalman Filter to mitigate noise and uncertainties.

Limitation of the existing solutions: While existing IMU-based solutions suffer from problems like low accuracy, the RF-based studies require multiple anchor nodes. This makes these solutions inapplicable in scenarios like in Fig. 1, which motivates us to design a single anchors-based and infrastructure-less localization solution. Reference [27] is closest to our work, however, the solution uses IMU sensors along with UWB radios and therefore does not entirely overcome the above limitations.

### C. Our contributions

In this paper, our primary contribution is as follows. We propose the development of a UWB-based localization system using a single anchor node. This is obtained by measuring the distances and angles between the anchor and the tags. For the distance estimation, we measure the time-of-flight based on the two way ranging (TWR) method [28], whereas for angle measurements, we propose two techniques - the first one uses AoA measurement using an antenna array, whereas the second approach relies on spinning the anchor transceiver using a motor and figuring out the angle at which the tag's RSSI value is maximal. We conduct thorough experimentation of the developed localization system in diverse real-world scenarios using DWM1001 UWB chips [29]. This includes assessing the system's performance in both Line of Sight (LOS) and Non-Line of Sight (NLOS) environments; through experimentation, we show that the proposed approaches archive a

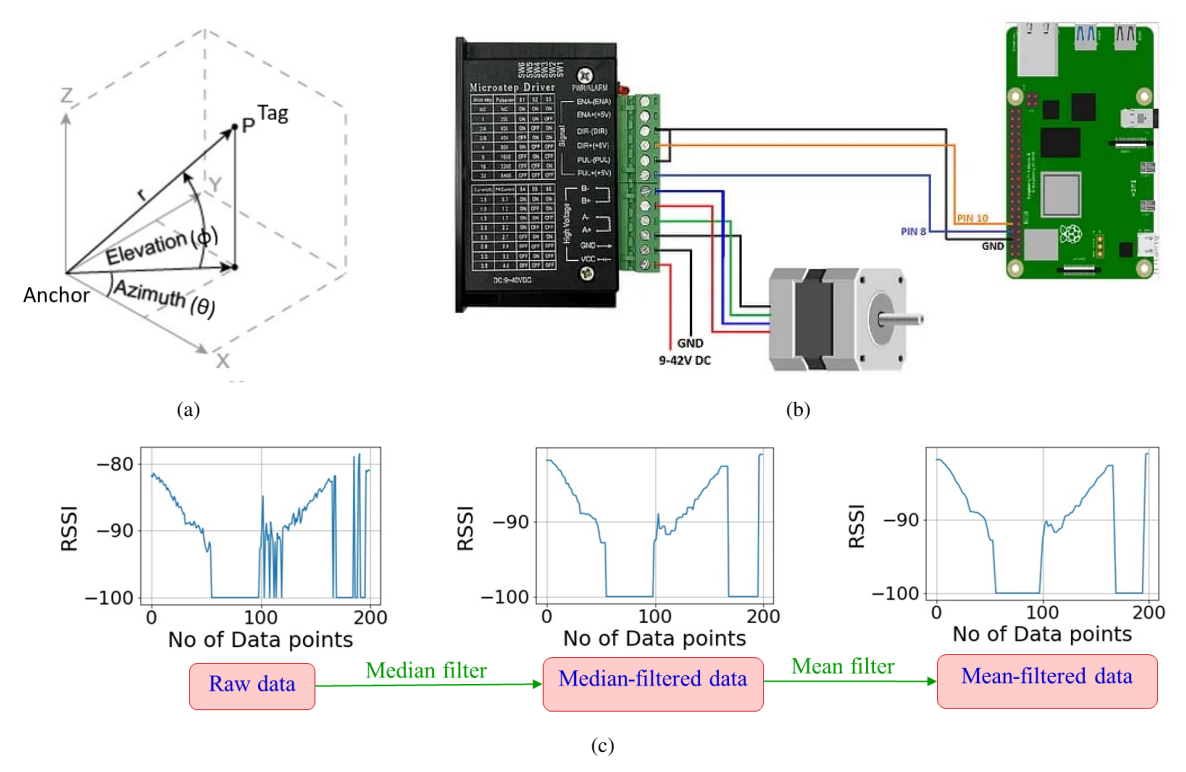


Fig. 3: (a) Axis convention used in our study. (b) Our setup for angle estimation using MRBAD method. (c) Different stages of the data filter pipeline.

distance estimation accuracy of < 1 m, whereas the angle measurement errors remain below  $10^{\circ}$ .

The remainder of the paper is organized as follows. Section II presents our proposed framework for localizing the tags using SAL. Section III summarizes our experimental setup. Experimental evaluation and results are summarized in section IV. Section V then concludes the paper.

# II. PROPOSED FRAMEWORK

In order to localize a UWB tag with respect to an anchor node using SAL, we need to measure the distance and angle between the tag and the anchor. For distance measurement we use the Two Way Ranging (TWR) [28], [30]–[32] scheme that provides Time-of-flight (ToF) in between the transceivers, which can be multiplied by the speed of light to get the distance estimation. For angle measurements, we use two techniques: the first one uses the phase difference captured by an antenna array, whereas the second technique rotates the anchor node and measures the angle from which it receives the tag's signal with maximum strength. Below we briefly summarize these approaches.

# A. Time-of-flight measurement

Estimating the distance between a pair of transceivers is challenging in RF mainly due to the clock offsets and clock drifts between the transceivers, which can introduce errors in position estimation. To alleviate these issues, the TWR mechanism exchanges three control messages between the anchor and the tag to minimize the clock offsets and drifts, as shown in Fig. 2(a). From this figure, it can be derived that

the ToF in between the anchor (i.e. device A) and the tag (i.e. device B) is  $\frac{(R_A - D_B) + (R_B - D_A)}{4}$ , which eliminates the clock offsets and greatly alleviates the clock drifts [28].

### B. Angle measurement

Apart from distance estimation, in SAL the anchor node also needs to estimate the angle of the tags to locate them, as shown in Fig. 3(a). For our study, we measure the angles (i.e. the azimuthal angle  $\theta$  and elevation angle  $\phi$ ) using the following two methods.

Angle of Arrival (AoA) method: The AoA technique involves the use of multiple antennas or antenna arrays at the receiver end. By measuring the phase differences or time delays of the signals received by each antenna, the AoA can be estimated. In Fig. 2(b) we describe a simple AoA measurement technique using an antenna array  $a_0-a_{N-1}$ . Suppose the transmitter sends a sinusoidal signal  $s(t)=x(t)\cos(2\pi ft)$ , whereas the receiver array receives  $y_0(t)-y_{N-1}(t)$ . Then the frequency responses of the received signals at  $a_0-a_{N-1}$ 

are given by: 
$$Y(f) = \begin{pmatrix} S(f)e^{j0} \\ S(f)e^{j\phi} \\ \dots \\ S(f)e^{j(N-1)\phi} \end{pmatrix}$$
, where  $S(f)$  is the

attenuated version of s(t),  $\phi = \frac{2\pi}{\lambda} d\cos\theta$ , where  $\lambda$  is the signal wavelength, d is the inter-antenna distance and  $\theta$  is the AoA (which is unknown). Therefore, given the received signals at the antenna arrays, the unknown  $\theta$  can be estimated by a brute-force technique.

Maximal RSSI Based Angle Determination (MRBAD) method: In this method, the anchor rotates along a specific

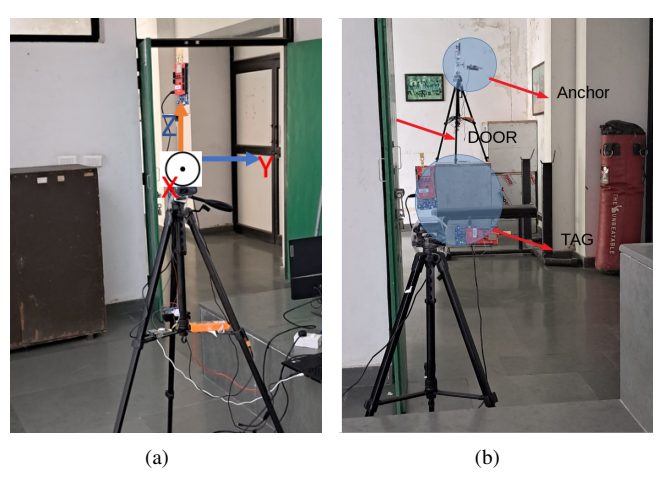


Fig. 4: (a) Axis convention along with the (b) experimental setup for the 3d localization using the AoA method.

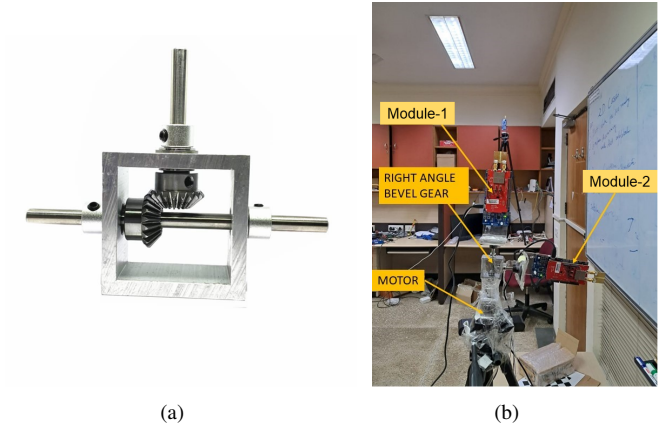


Fig. 5: The MRBAD method uses (a) a bevel gear to rotate the UWB modules. (b) Experimental setup for 3d localization using the MRBAD method.

axis (say z-axis), and the angle at which the received signal strength (RSSI) at the tag is maximum is measured. This angle provides information about the tag's angle in the x-y plane. In this study, the anchor is mounted on the stepper motor [33] having a step size of 1.8°. In order to accurately manage the motor speed, a Raspberry Pi [34] is configured to spin the motor by 1.8° per 200 milliseconds, resulting in one full 360° rotation taking approximately 40 seconds. The setup is illustrated in Fig. 3(b). On top of the motor, a UWB Decawave QM33120W board is mounted with the help of a shaft. One end of the shaft is fixed to the motor, and the other end is fixed to the UWB chip. Once the full rotation of 360° is performed, the anchor is made to rotate in the opposite direction in order to avoid wire entanglement.

Once the RSSI data is acquired, we implement the following steps in order to find the appropriate angle, which is illustrated in Fig. 3(c). The hypothesis behind the scheme is that the RSSI value between the tag and anchor is maximum when the tag antenna is perfectly aligned with the anchor. The hypothesis is facilitated by the use of directional antenna on the anchor side. Initially, the data undergoes a median filter, which is a type of signal processing filter used to remove noise

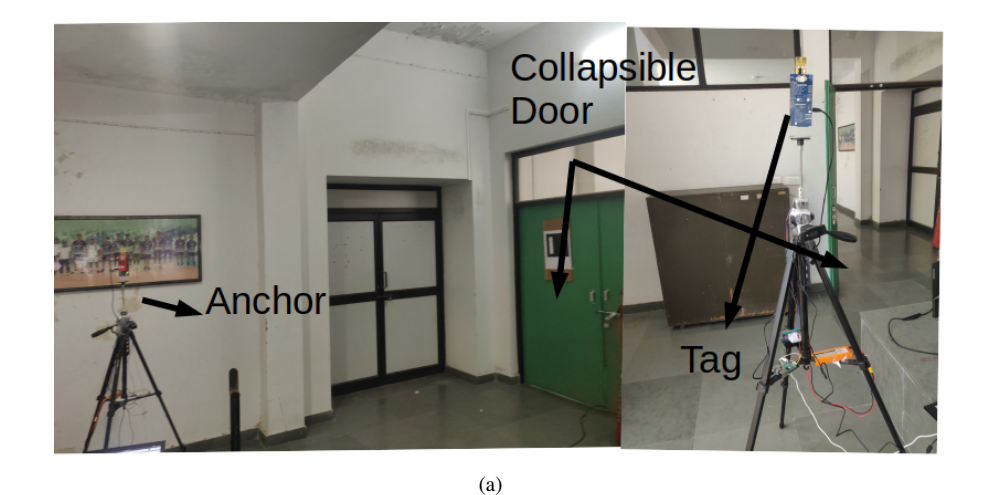
and outliers from a signal [35]. This effectively removes the spikes and other undesirable artifacts that may be caused due to multipaths, and provides a cleaner representation of RSSI values, as shown in Fig. 3(c). Additionally, a mean filter is applied to further reduce the noise in the data [36]; the output of the mean filter is also shown in Fig. 3(c). Next a peak detection algorithm is used to determine the position where the maximum RSSI value is observed, which is then converted into an appropriate angle by multiplying with the step size of the motor (i.e. 1.8°). In case when multiple peaks are detected, the algorithm favors the position where there is a steady rise and fall of the RSSI values.

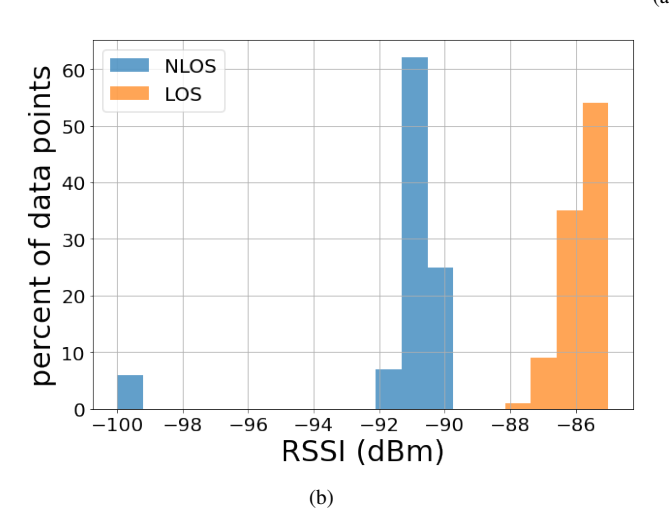
# III. EXPERIMENTAL SETUP

For our experimental setup, we use Decawave QM33120WDK1 kit [29] that consists of two boards, and QM33110W. The QM33120W QM33120WDK1 firmware performs accurate time-stamping of the signal by minimizing the processing delay, which is crucial for accurate ToF measurements. For localizing the tags using the AoA method, we use the QM33120W device as an anchor; the choice of the anchor is driven by its two directional antennas, which enables us to determine the angle using AoA technique. These antennas are separated by a distance of  $\frac{\lambda}{2}$ , where  $\lambda$  is the signal wavelength. The UWB radios are made to operate in channel 9 having a frequency of 7987.2 MHz, thus the distance between the antennas is 1.88 cms. The tag (i.e. the QM33110W device) on the other hand has one omnidirectional antenna.

In the case of localization in 3D, both the anchor and the tag consist of two UWB modules (QM33120W for the anchor, whereas QM33110W for the tags) placed in orthogonal planes. The first module is placed along the z-axis in xy plane, the purpose of this module is to measure the azimuthal angle of the tag's position. The second module is placed along the y-axis in xz plane, which measures the elevation angle. The setup is shown in Fig. 4.

For localizing the tags using the MRBAD method, we use two UWB modules (i.e. the QM33120W devices) that are mounted on a single rotating platform, as the anchor node. One module rotates across the z-axis, while the other rotates across the y-axis. A single stepper motor is used for transferring rotation powers and regulates both modules using a "spiral bevel gear", allowing the simultaneous rotation in two distinct orthogonal planes. The gear ratio is set to 1:1 such that the angular displacement of both modules is identical in their respective planes. At the tag end, two transceivers (i.e. QM33110W devices ) are strategically positioned in orthogonal directions - one of them is associated with the horizontal QM33120W module, whereas the other one is linked to the vertical module. The module rotating along the z-axis is used to find the azimuthal angle while the other one is responsible for finding the elevation angle. The tag sends data to both the modules every 200 ms. The corresponding RSSI values at both the modules and ToF are captured and





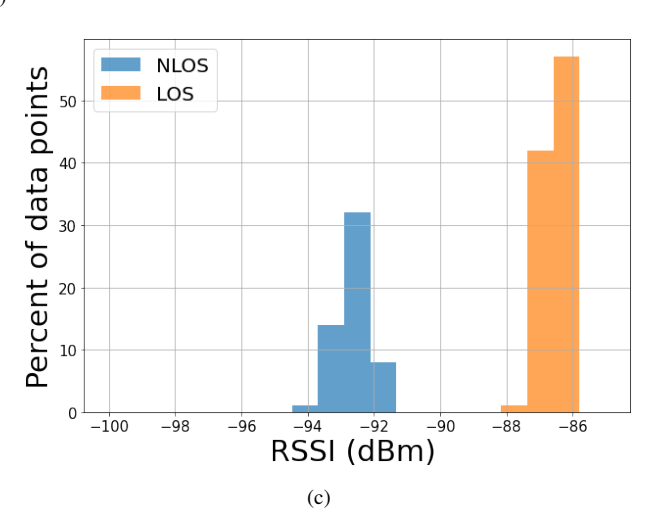


Fig. 6: (a) Our experimental setup. Comparison of RSSI where the transceivers are kept at a distance of (b) 8.5 meters and (c) 11.4 meters.

stored on the onboard Raspberry Pi [34]. The experimental setup is shown in Fig. 5.

The experimental setup is mounted on a tripod stand. A Lipo battery of 11.1 V is used to supply the power to both the stepper motor and the Raspberry pi. The relevant data is collected from the anchor and later transferred to a standalone PC for analysis. The anchor's position remains static throughout the experiments, whereas the tag positions are deliberately randomized. To compare the accuracy of the proposed localization techniques, the ground truth measurements of the tag locations are done manually.

Our experiments cover a spectrum of conditions, encompassing both LOS and NLOS scenarios. The NLOS condition is achieved by passing the signal through a collapsible door, emulating real-world scenarios where obstacles may obstruct direct LOS communication. One such setup is shown in Fig. 6(a). Once the door is opened the system obtains LOS data, whereas when the door is closed NLOS data are collected.

# IV. EXPERIMENTAL EVALUATION

In this section, we evaluate our experimental outcomes for both LOS and NLOS scenarios. We briefly discuss our results for 2D localization first, and then move on to the 3D experiments in detail.

## A. Path loss using UWB radios

We first show the amount of transmission loss using the UWB radios both in the case of LOS and NLOS scenarios. Fig. 6(b)-(c) show the distribution of RSSI values received at different positions. From this figure, we can observe that in NLOS scenario, the door in the middle of the transceivers results in  $\sim$ 5-6 dB loss. We can also observe that the RSSI values drop below -92 dbm beyond 11-12 meters, which limits the operational area of our experiment. Notice that this limitation is mainly due to the limited transmit power of the UWB radios because of the FCC regulations [37], however, in our experiments, our primary goal is to study the potential of the UWB radios in SAL scenarios.

## B. Experimental results for 2D localization

**Results using AOA method:** In case of 2D localization, an anchor and a tag are mounted on two tripod stands with known height. We conduct these experiments in five positions; for the first four positions the transceivers are placed at two sides of a door – closing the door imitates the NLOS scenario.

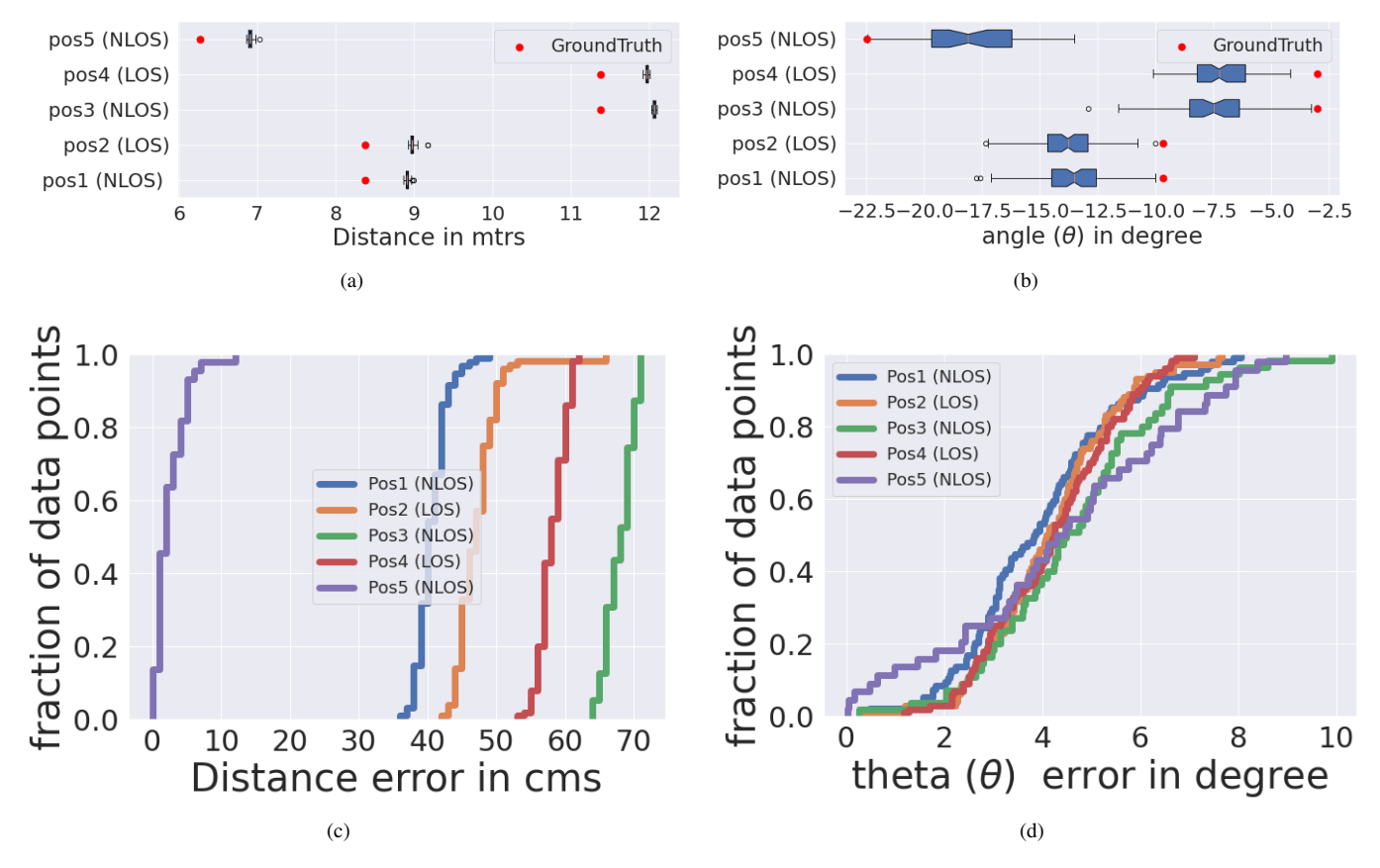


Fig. 7: Experimental results of (a)-(c) distance and (b)-(d) angular errors for 2D localization in case of LOS and NLOS scenarios using AoA method.

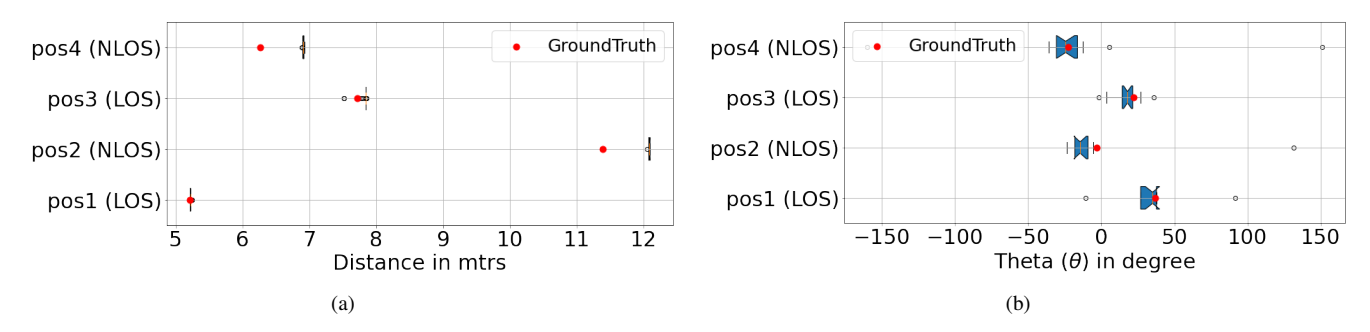


Fig. 8: Experimental results of (a) distance and (b) angular errors for 2D localization in case of LOS and NLOS scenarios using MRBAD method.

For the fifth position, the transceivers are placed on two sides of a wall. For each position, 100 data points are collected for distance and AOA estimation.

Fig. 7 shows the comparison of distance and angular errors in case of LOS and NLOS scenarios. Fig. 7(a)-(c) show that for all these cases, the distance error remains below 80 cm, whereas the median error remains below 70 cm. From Fig. 7(b)-(d) we can also observe that for 80% of the points, the angular error remains below 6°. In fact, the maximum angular error observed in both LOS and NLOS scenarios remains below 10°. As mentioned earlier, for position 5 there is a wall in between the transceivers; the median ranging and angular errors in this case are 3 cm and 4.38° respectively.

Results using MRBAD method: For estimating the angle

between the anchor and the tag using the MRBAD method, the anchor module is attached to a motor, enabling it to rotate a full 360° in ~40 seconds. The RSSI values are then passed through the processing pipeline as shown in Fig. 3(c). During each rotation, a total of 200 data points are collected. The motor continues to rotate for a duration of 9-10 minutes, allowing us to collect a substantial amount of data for multiple rounds of rotations. We then take the *median* of the measured angles in these rounds, to get rid of the outliers. Fig. 8 shows the results of our experiments. From this figure, we can observe that the ranging errors in case of NLOS vary in between 65-79 cm, whereas the angular errors vary between 0.82°-7.79°. In fact, the results do not change significantly using the AoA and MRBAD methods.

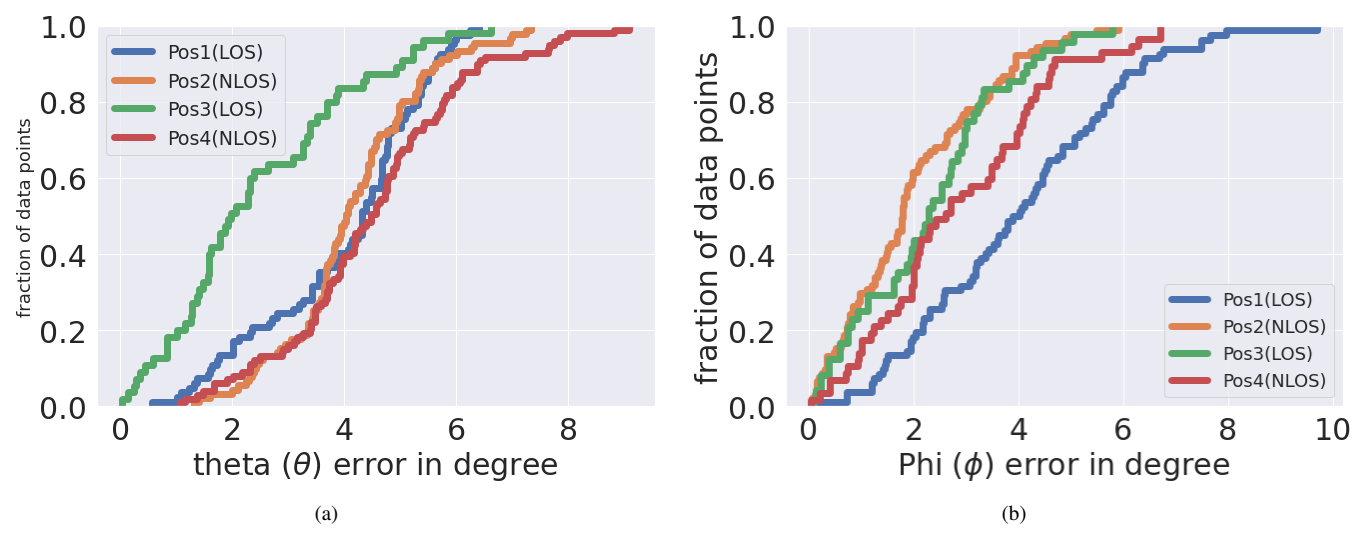


Fig. 9: Experimental results of angular errors for 3D localization in case of LOS and NLOS scenarios using AoA method.

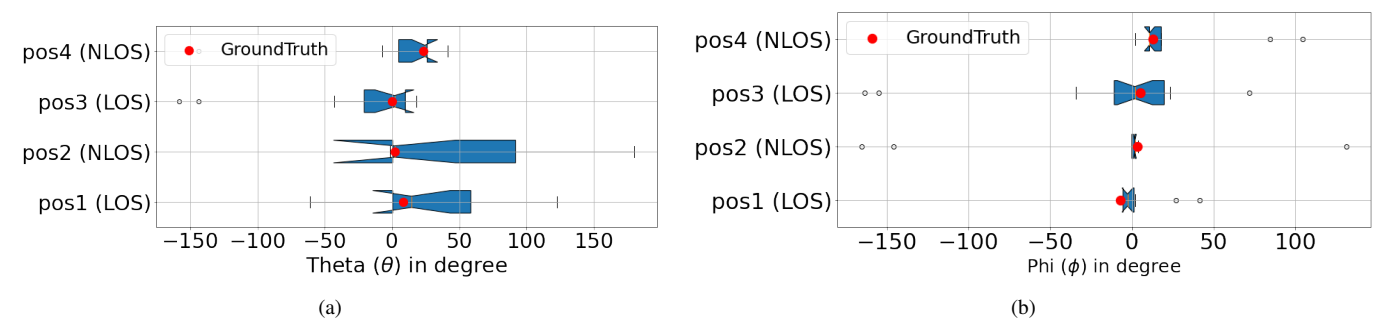


Fig. 10: Experimental results of angular errors for 3D localization in case of LOS and NLOS scenarios using MRBAD method.

# C. Experimental results for 3D localization

**Results using AoA method:** For localizing the tags in 3D, the anchor node consists of two QM33120W modules placed at an angle of  $90^{\circ}$ , so that we can uniquely localize the tags by estimating their angles in both xy and yz planes w.r.t. the anchor. We place a tag at different random positions inside a room; for each position, 100 data points were collected. The vertical QM33120W module measures the angle in the horizontal plane (i.e.  $\theta$ ), whereas the horizontal one measures the angle in the vertical plane (i.e.  $\phi$ ). The distance measurement is measured only from the vertical module.

Fig. 9 shows the comparison of LOS and NLOS scenarios. We show only the angular errors, as the ranging errors are very similar to those of 2D localization. From Fig. 9, we can observe that the median angular errors remain between  $2^{\circ}-5^{\circ}$  for various positions. In fact, for 80% of the measurements, the angular errors lie between  $3^{\circ}-6^{\circ}$ .

**Results using MRBAD method:** For localizing the tags using the MRBAD method, we utilize two QM33120W modules that are mounted on a rotating platform to imitate an anchor node, as mentioned in section III. The experimental results are shown in Fig. 10. Using the MRBAD method as well, we can observe that the angular errors are within a satisfactory range; the errors corresponding to  $\theta$  and  $\phi$  lie

within 6.27° and 4.61° respectively. The conclusions drawn from these results are summarized as follows:

- The range estimation using TWR technique performs extremely well, restricting the median error within 70 cm. The angle measurements using AoA and MRBAD methods are also pretty accurate both in LOS and NLOS scenarios, with a median angular error  $< 6^{\circ}$  for both  $\theta$  and  $\phi$ .
- ➤ For all the measurements, the maximum ranging error remains well below 1 m, whereas the angular errors always lie below 10°.
- ➤ There doesn't seem to be a significant loss in the localization accuracy in the LOS and NLOS cases, which shows the robustness of the TWR as well as the AoA and MRBAD mechanisms.
- ➤ The experimental distance measurements are generally close to the ground truth values, indicating that the TWR method can effectively resolve the multipath effects and can provide a reasonable level of ranging accuracy. The angular estimations are slightly off as compared to the ground truth values, however, still remain below 10°.

## D. Comparison of the AoA and MRBAD schemes

We now compare these two schemes along with their pros and cons. From our experiments, we can observe that the AoA method is faster and slightly more accurate as compared to the MRBAD one. The resolution of the MRBAD method is kept at 1.8° for our experiments; this resolution can be improved by decreasing the step size of the motor, at the cost of slower localization speed. This may be acceptable for scenarios where the tags have slow mobility, however, is problematic for fast-moving scenarios. In those scenarios, the AoA technique is more suitable. The requirement of motors also makes the MRBAD transceivers bulkier. On the other hand, the AoA schemes require an antenna array, whereas the MRBAD solution can work with isolated antennas.

### V. CONCLUSIONS AND DISCUSSION

In this study, we explore two approaches for tracking the UWB tags using a single anchor node, by combining the distance measurements from two-way ranging and the angle information in between the transceivers. The experiments conducted in this research showcase high level of accuracy in estimating angles and distances between anchor and tags. The TWR technique proves to be highly effective in both Line-of-Sight (LOS) and Non-Line-of-Sight (NLOS) scenarios, with an average ranging error of less than 1 m. The proposed methods for angle measurements in between the anchors and tags also demonstrate a high level of accuracy, with an angular error of less than 10°.

Our measurement results highlight the system's potential and robustness in developing localization solutions in any infrastructure-less scenarios, like search and rescue operations, emergency management situations, etc. In future, we envision enhancing the flexibility of the anchor system to further improve the localization capabilities. We also want to make this system more lightweight, so that the transceiver units can be mounted on any platform like drones or UAVs that can localize the tags in any specific locations as needed.

# ACKNOWLEDGEMENTS

This research was supported by the IIT Kanpur Initiation Grant IITK/CS/2021164 and IITK-Rice University Strategic Collaboration Award IITK/DOIR/2023227.

#### REFERENCES

- [1] J. Yi et al., "Imu-based localization and slip estimation for skid-steered mobile robots," in IEEE/RSJ IROS, 2007, pp. 2845-2850.
- [2] L. Huang, "Review on lidar-based slam techniques," in CONF-SPML, 2021, pp. 163-168.
- [3] S. Brassai et al., "Radio frequency (rf)-based, real-time, indoor localization system for unmanned aerial vehicles and mobile robot applications," Acta Polytechnica Hungarica, vol. 17, pp. 19-40, 01
- [4] "Six firemen died during rescue operations since 2016: Delhi fire service," 2020, accessed on 2023-09-24. [Online]. Available: https:// timesofindia.indiatimes.com/city/delhi/six-firemen-died-during-rescueoperations-since-2016-delhi-fire-service/articleshow/73074626.cms
- "4 firemen among 9 killed in kolkata high-rise inferno," 2021, accessed on 2023-09-24. [Online]. Available: //timesofindia.indiatimes.com/city/kolkata/four-firemen-among-9people-killed-in-kolkata-high-rise-inferno/articleshow/81402615.cms

- [6] "Fatal firefighter injuries in the united states." 2023, 2023-09-24. accessed on [Online]. able: https://www.nfpa.org/News-and-Research/Data-research-andtools/Emergency-Responders/Firefighter-fatalities-in-the-United-States
- "The ordinary heroes of the taj," accessed on 2023-09-24. [Online]. Available: https://hbr.org/2011/12/the-ordinary-heroes-of-the-taj
- [8] F. Höflinger et al., "Indoor-localization system using a micro-inertial measurement unit (imu)," in EFTF, 2012, pp. 443-447.
- [9] H. Guo et al., "Indoor positioning based on foot-mounted imu," Bulletin of the Polish Academy of Sciences. Technical Sciences, vol. Vol. 63, nr 3, pp. 629-634, 2015.
- [10] R. Zhang et al., "Indoor localization using a smart phone," in IEEE SAS, 2013, pp. 38-42.
- [11] Q. Xu et al., "Idyll: Indoor localization using inertial and light sensors on smartphones," in ACM UbiComp, 2015, pp. 307-318.
- [12] C. Lu et al., "Indoor positioning system based on chest-mounted imu," Sensors, vol. 19, no. 2, 2019.
- M. Altini et al., "Bluetooth indoor localization with multiple neural networks," in IEEE ISWPC, 2010, pp. 295-300.
- [14] P. Vorst et al., "Indoor positioning via three different rf technologies," in European Workshop on RFID Systems and Technologies, 2008.
- [15] P. Bahl et al., "RADAR: an in-building rf-based user location and tracking system," in IEEE INFOCOM, 2000, pp. 775–784.
- [16] M. Youssef et al., "The horus location determination system," Wireless Networks - WINET, vol. 14, pp. 357-374, 06 2008.
- M. Ramadan et al., "Nlos identification for indoor localization using random forest algorithm," in WSA, 2018, pp. 1-5.
- [18] J. Cunha et al., "Using a depth camera for indoor robot localization and navigation," DETI/IEETA-University of Aveiro, Portugal, vol. 27, no. Jun, p. 6, 2011.
- [19] B. Hanssens et al., "An indoor localization technique based on ultrawideband aod/aoa/toa estimation," in IEEE APSURSI, 2016, pp. 1445-
- [20] P. Meissner et al., "Accurate and robust indoor localization systems using ultra-wideband signals," CoRR, vol. abs/1304.7928, 2013. [Online]. Available: http://arxiv.org/abs/1304.7928
- [21] P. Dabove et al., "Indoor positioning using ultra-wide band (uwb) technologies: Positioning accuracies and sensors' performances," in IEEE/ION PLANS, 2018, pp. 175-184.
- [22] A. Poulose et al., "Uwb indoor localization using deep learning 1stm networks," Applied Sciences, vol. 10, no. 18, 2020.
- [23] Y. Rahayu et al., "Ultra wideband technology and its applications," in IFIP WOCN, 2008, pp. 1-5.
- [24] R. I. Vitanov et al., "A state-of-the-art review of ultra-wideband localization," in ICEST, 2022, pp. 1-4.
- [25] A. Poulose et al., "Hybrid indoor localization using imu sensors and smartphone camera," Sensors, vol. 19, no. 23, 2019.
- [26] V. Malyavej et al., "Indoor robot localization by rssi/imu sensor fusion," in ECTICon, 2013, pp. 1-6.
- [27] A. Dhekne et al., "TrackIO: Tracking first responders Inside-Out," in
- USENIX NSDI, 2019, pp. 751–764.
  [28] D. Neirynck *et al.*, "An alternative double-sided two-way ranging method," in WPNC, 2016, pp. 1-4.
- [29] Qorvo. Accessed on 2023-09-24. [Online]. Available: https://www. qorvo.com/products/p/QM33120WDK1
- [30] I. Domuta et al., "Two-way ranging algorithms for clock error compensation," IEEE Transactions on Vehicular Technology, vol. 70, no. 8, pp. 8237–8250, 2021.
- [31] S. Lanzisera et al., "Radio frequency time-of-flight distance measurement for low-cost wireless sensor localization," IEEE Sensors Journal, vol. 11, no. 3, pp. 837-845, 2011.
- [32] K. A. Horváth et al., "Passive extended double-sided two-way ranging algorithm for uwb positioning," in ICUFN, 2017, pp. 482-487.
- "Stepper motor," accessed on 2023-09-24. [Online]. Available: https://reprap.org/wiki/NEMA\_17\_Stepper\_motor
- [34] "Raspberry pi," accessed on 2023-09-24. [Online]. Available: https:// www.raspberrypi.com/products/raspberry-pi-4-model-b/specifications/
- [35] G. George et al., "A survey on various median filtering techniques for removal of impulse noise from digital image," in ICEDSS, 2018, pp. 235-238.
- [36] u. erkan et al., "An iterative mean filter for image denoising," IEEE Access, vol. 7, pp. 167847–167859, 2019.
- [37] G. Breed, "A summary of fcc rules for ultra wideband communications," High Frequency Electronics, pp. 42-44, 2005.